Radio-frequency magnetron sputtering deposition process for In_2O_3:H transparent conductive oxide films for application in Cu(In,Ga)Se_2 solar cells

Marina Alves , Daniel Brito , Joaquim Carneiro , Vasco Teixeira , Sascha Sadewasser

PII: S0040-6090(23)00170-0
DOI: https://doi.org/10.1016/j.tsf.2023.139840
Reference: TSF 139840

To appear in: *Thin Solid Films*

Received date: 24 June 2022
Revised date: 31 March 2023
Accepted date: 6 April 2023

Please cite this article as: Marina Alves , Daniel Brito , Joaquim Carneiro , Vasco Teixeira , Sascha Sadewasser , Radio-frequency magnetron sputtering deposition process for In_2O_3:H transparent conductive oxide films for application in Cu(In,Ga)Se_2 solar cells, *Thin Solid Films* (2023), doi: https://doi.org/10.1016/j.tsf.2023.139840

Highlights

- Growth of In_2O_3:H (IOH) using a gas mixture of Ar/H_2 as a H-doping alternative.
- The O_2 partial pressure strongly influenced the sheet resistance.
- No significant changes in the average visible transmittance (AVT).

Radio-frequency magnetron sputtering deposition process for In_2O_3:H transparent conductive oxide films for application in Cu(In,Ga)Se_2 solar cells

Marina Alves[a,b], Daniel Brito[a], Joaquim Carneiro[b], Vasco Teixeira[b], Sascha Sadewasser[a]

(a) International Iberian Nanotechnology Laboratory, Av. Mestre José Veiga s/n, 4715-330, Braga, Portugal,
(b) Centre of Physics of Minho and Porto Universities (CF-UM-UP), Azurém Campus, 4800-058 Guimarães, Portugal

Abstract

Typical Cu(In,Ga)Se_2 solar cells are deposited on an opaque molybdenum back contact. However, for applications such as bifacial, semi-transparent or tandem solar cells a transparent back contact is required, for which various transparent conductive oxides have been tested, such as indium- or fluorine-doped tin oxide, and hydrogen-doped indium oxide. Here, a radio-frequency magnetron sputtering deposition process for In_2O_3:H (IOH) is investigated, where H is supplied from a Ar/H_2 (5%) mixed gas and oxygen is pulsed during the entire deposition at room temperature. After deposition, the films are post-annealed in vacuum to optimize their optoelectronic properties. The oxygen plays an important role for the optoelectronic properties, where a high content of oxygen allows higher transparency but also increases the film sheet resistance. Optimum oxygen and Ar/H_2 partial pressures of 3.2×10^{-2} Pa and 13×10^{-2} Pa, respectively, were found, producing IOH films with average visible transparency of 87% and sheet resistance after annealing of 19 Ohm/sq.

Keywords: Indium oxide; Hydrogen-doped indium oxide; Sputtering; Transparent conductive oxide; Sheet resistance

1. Introduction

Due to the limited nature of fossil fuels, renewable energy sources have become increasingly needed, especially photovoltaic technologies. Semi-transparent photovoltaic technologies combine the benefits of visible light transparency and light-to-electricity conversion [1], which can be integrated into windows to be used in buildings. Building-integrated photovoltaics (BIPV) is a general term used for solar cells that are directly integrated into building elements, such as windows, walls and roofs [1].

Thin-film $Cu(In,Ga)Se_2$ (CIGS) solar cells have high conversion efficiency (23.35% [2]), direct bandgap, high absorption coefficient, low temperature coefficient, less material waste [3,4], and stability among all thin-film-based solar cells [5], becoming an interesting candidate for this type of application. CIGS solar cells commonly use Mo as back contact. To use a transparent conductive oxide (TCO) as a transparent back contact, some requirements are needed, such as (1) creating an ohmic contact to the absorber, (2) being highly transparent and, (3) exhibiting a low sheet resistance [6]. Several TCO materials have been investigated as a potential transparent back contact for CIGS solar cells, such as ZnO:Al, SnO:F and In_2O_3:Sn. However, these materials present significant performance losses when compared to standard Mo back contact due to the high temperature used for CIGS deposition [7]. Furthermore, for ZnO:Al and SnO:F, the formation of Ga_2O_3 was observed, which can be detrimental at the back contact/CIGS interface [6,7].

Koida *et al.* [8] developed hydrogen-doped In_2O_3 (In_2O_3:H, IOH) films by sputtering at room temperature using water vapor as dopant source, followed by an annealing step at 200 °C to crystallize the amorphous film, producing films with high mobility and high near-infrared transparency. Commonly, In_2O_3 films have polycrystalline structures when deposited without intentional heating, however, by introducing H_2O vapor or H_2 during the growth, the structure changes to amorphous phases [9,10]. High conductivity in TCO films can be achieved by

enhancing the free carriers (i.e., by increasing oxygen vacancies) or the carrier mobility (i.e., by reducing the carrier scattering) [11]. The H-doping reduces carrier scattering in the crystallized In_2O_3, and the crystallization eliminates O deficiency and generates H^+ that acts as a singly charged donor [12].

IOH has been used as TCO in silicon heterojunction [13–16] and CIGS solar cells [10,17]. Jäger *et al.* investigated amorphous IOH as TCO deposited using water vapor or H_2 gas during the sputtering process, in which the power conversion efficiency of CIGS solar cells improved from 15.7% to 16.2% by replacing ZnO:Al with IOH doped with water vapor [10]. Keller *et al.* [6] were the first to evaluate the use of IOH as a transparent back contact in chalcopyrite solar cells, producing an (Ag,Cu)(In,Ga)Se_2 (ACIGS) solar cell with an efficiency of 16.1%. Keller *et al.* [7] also reported the use of IOH as a transparent back contact in bifacial ACIGS solar cells, achieving efficiencies of 11 % at front and 6 % at back side illumination. In most works, H-doping is achieved by supplying water vapor during deposition. However, the use of water vapor as dopant source presents challenges regarding its precision, stability, reproducibility and industrial application [11,18]. To avoid these issues, gases can be used, allowing more control during the process.

Therefore, the development of an IOH transparent back contact to replace Mo, integrated with ultrathin or micro-sized CIGS technology could be a successful approach for semi-transparent photovoltaics. The aim of this work is to develop a radio-frequency magnetron sputtering deposition process for IOH films using a gas mixture of Ar/H_2 and pulsed oxygen to be applied as a transparent conductive oxide in CIGS solar cells.

2. Materials and methods

IOH films were deposited by RF sputtering from a 2-inch ceramic In_2O_3 target without intentional substrate heating. Hydrogen doping was attained by introducing a gas mixture of Ar/H_2 (5% of H_2). The sputtering conditions were varied, including O_2 and Ar/H_2 partial pressures and film thickness. The films were deposited on 1 mm thick soda-lime glass (Menzel-Gläser) at room temperature by RF sputtering with a power of 30 W, corresponding to a power density of 1.5 W/cm^2. The base pressure of the chamber was less than 5×10^{-4} Pa, and the total working pressure (Ar, Ar/H_2 and O_2) during the deposition varied between 4.8 – 5.7×10^{-1} Pa. The oxygen partial pressure ($p(O_2)$) varied between 2.1×10^{-2} (0.5 sccm oxygen flow) and 3.9×10^{-2} Pa (2 sccm), and the Ar/H_2 partial pressure ($p(Ar/H_2)$) between 3.1×10^{-2} (0.8 sccm Ar/H_2 flow) and 1.3×10^{-1} Pa (1.2 sccm). Due to the limitations of the mass flow controller, a flow below 0.5 sccm could not be controlled reliably. Therefore, to achieve lower oxygen content in the sputtering atmosphere, oxygen was pulsed into the system for one minute every two minutes. After deposition, the films were post-annealed in vacuum at 200 °C for one hour.

Four-point probe measurements (CMT-SR2000NW) were conducted to determine the sheet resistance of the IOH films. Transmittance measurements were acquired by using a Perkin Elmer Lambda 950 spectrophotometer, and the average visible transmittance (AVT) was calculated using the wavelength range from 380 nm to 780 nm. The crystalline structure of IOH films was investigated by X-ray diffraction (XRD) using X'Pert Pro MRD system.

3. Results and Discussion

To investigate the oxygen partial pressure variation behavior, the films were deposited without Ar/H_2 supply, and thickness of 180 nm. Fig. 1a shows the change of the sheet resistance (Rsh) of the as-deposited and annealed In_2O_3 films. In the case of as-deposited

films, for low $p(O_2)$ until 3.2×10^{-2} Pa, the Rsh decreases, and for higher $p(O_2)$ the Rsh increases. After annealing, the Rsh increases for all films, showing the same evolution as a function of $p(O_2)$. Although the sheet resistance is expected to increase for higher oxygen content, the increase before and after the optimum $p(O_2)$ could be related to film structure and morphology, and oxygen vacancies, respectively. The oxygen partial pressure will influence the defects related to oxygen deficiencies and the crystalline volume fraction of the amorphous film, affecting its properties [9]. Lower oxygen partial pressures will result in a more conductive but less transparent film, with smaller grain size, smoother and homogeneous surface and compact structure. However, if the partial pressure is too high, the opposite occurs and the film becomes more transparent, with better crystalline structure but insulating. During crystallization, structural rearrangements eliminate oxygen deficiency and generate H^+ that acts as a singly charged donor, substituting the oxygen vacancies, reducing the carrier density and improving the films' mobility. Thus, the presence of oxygen vacancies, which act as defects in the crystal lattice, can decrease conductivity, increase impurities and scattering leading to an increase in sheet resistance.

Fig. 1b shows the spectrally-resolved transmittance of these undoped In_2O_3 films in the visible region from 380 to 780 nm, after annealing. High optical transparency was obtained,

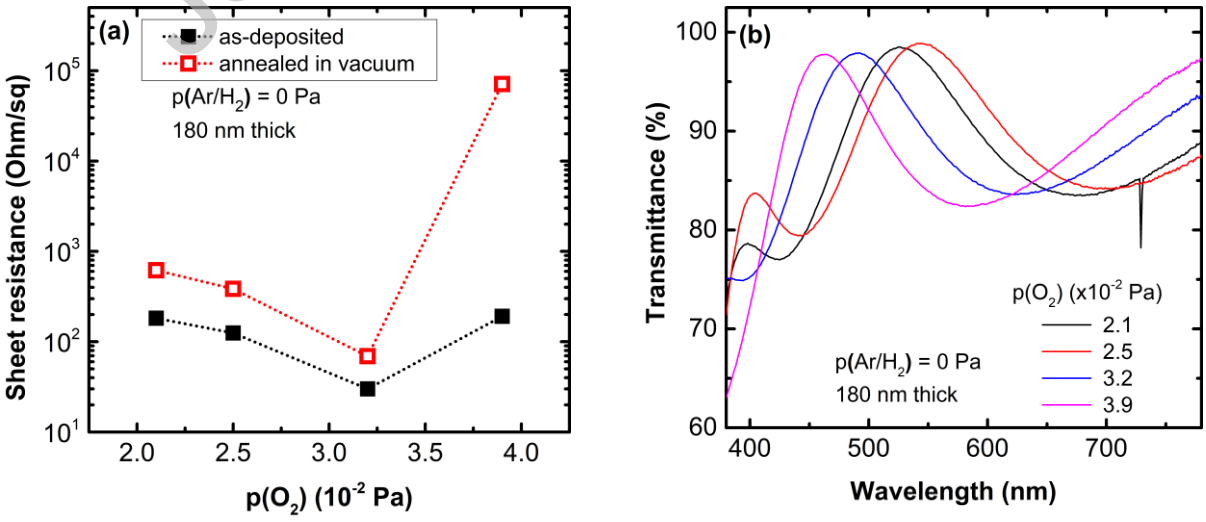

and the In_2O_3 films deposited with different $p(O_2)$ showed AVT of 87-88 %.

Fig. 1. (a) Sheet resistance as a function of oxygen partial pressure for as-deposited and annealed In_2O_3 films and (b) transmittance spectra of annealed In_2O_3 films.

To improve the conductivity of the In_2O_3 films, hydrogen-doping is introduced by adding Ar/H_2 at different partial pressures during the deposition, leading to IOH films. The $p(O_2) = 3.2\times10^{-2}$ Pa and film thickness of 180 nm were chosen. The sheet resistance (Fig. 2a) of as-deposited films drops significantly for $p(Ar/H_2) > 3\times10^{-2}$ Pa. At the same time, the Rsh only slightly increases after annealing for these samples, leading to their crystallization. Increasing the $p(Ar/H_2)$ should lead to higher H-doping and the elimination of oxygen vacancies, reducing the scattering and improving the film conductivity. However, for $p(Ar/H_2) = 3\times10^{-2}$ Pa, such increase in sheet resistance upon annealing is unusual and we do not yet have a proper explanation for this behavior. Fig. 2b shows the spectrally-resolved transmittance of annealed IOH films. The AVT of these IOH films is nearly identical to the

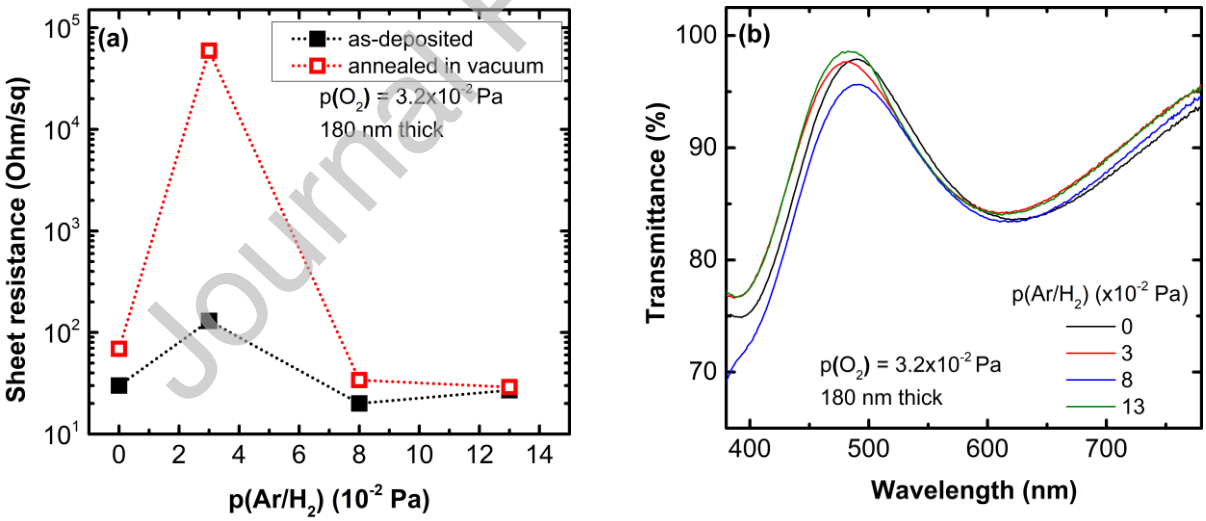

undoped films with values between 87 % and 89 %.

Fig. 2. (a) Sheet resistance as a function of Ar/H_2 partial pressure of as-deposited and annealed IOH films and (b) transmittance spectra of annealed IOH films.

Fig. 3 shows XRD patterns of IOH films grown at different $p(Ar/H_2)$. The as-deposited IOH films were mainly amorphous, while annealed IOH films are polycrystalline, with the

strongest diffraction peak for the (222) plane for all partial pressures. With increasing $p(Ar/H_2)$, also other diffraction peaks (such as for the (211), (400), (440) and (622) planes) become stronger. All peaks are in agreement with the In_2O_3 reference pattern (ICDD PDF 03-065-3170). The average crystallite sizes were estimated from the full width at half maximum (FWHM) values of the (222) diffraction peak using the Scherrer equation. With an increase of $p(Ar/H_2)$ from 3 to 8×10^{-2} Pa, the crystallite size increases from 18 to 30 nm, with no further increase for $p(Ar/H_2)$ of 13×10^{-2} Pa.

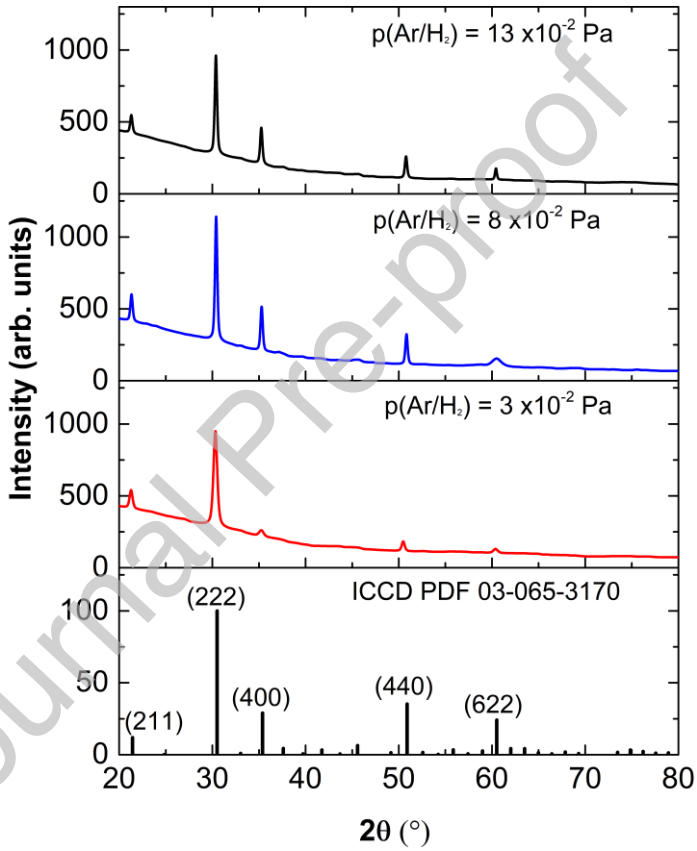

Fig. 3. X-ray diffraction patterns of annealed IOH films with different $p(Ar/H_2)$. Stick patterns of In_2O_3 reference (ICDD PDF 03-065-3170) are also shown for comparison (bottom).

To improve the electrical conductivity further, the film thickness was increased from 180 nm to 280 and 385 nm. As-deposited films with 280 and 385 nm presented Rsh of 18 and 14 Ohm/sq, respectively (Fig. 4a). After annealing, only the 385 thick IOH film presents Rsh below 20 Ohm/sq. The spectrally-resolved transmittance of annealed IOH films with different

thickness is shown in Fig. 4b. The AVT of IOH films with 180, 280 and 385 nm is 89 %, 89 % and 87 %, respectively.

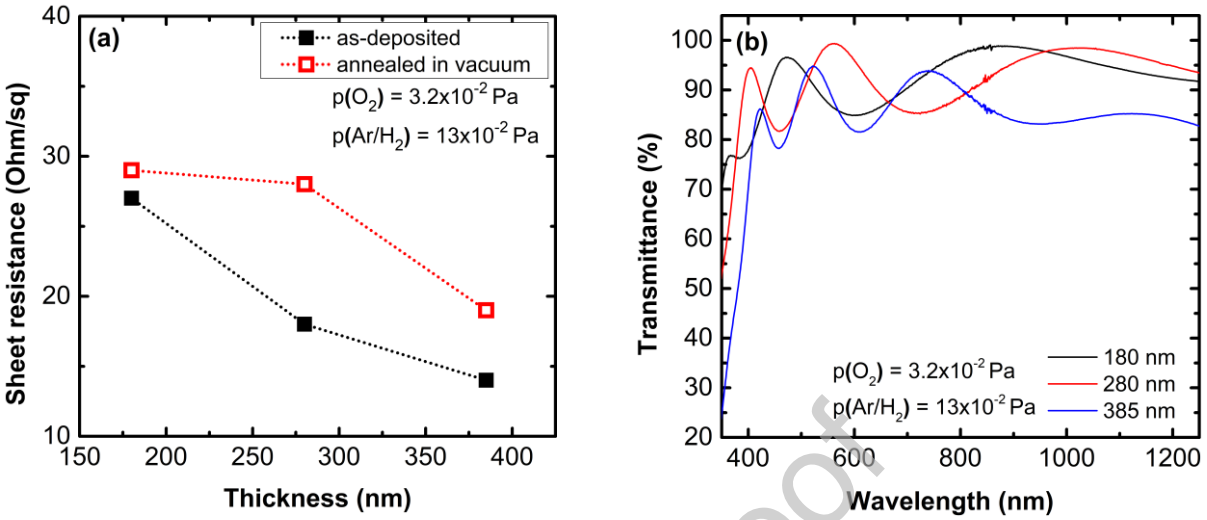

Fig. 4. (a) Sheet resistance as a function of thickness of as-deposited and annealed IOH films and (b) transmittance spectra of annealed IOH films.

The best balance between electrical and optical properties of IOH was obtained for a RF power density of 1.5 W/cm^2, $p(O_2)$ = 3.2×10^{-2} Pa, with oxygen pulses of one minute every two minutes, $p(Ar/H_2)$ = 13×10^{-2} Pa, total gas pressure of 5.4×10^{-1} Pa and thickness of 385 nm, resulting in an IOH film with average visible transparency of 87 % and sheet resistance before and after annealing of 14 and 19 ohms/sq, respectively.

4. Conclusion

We developed a RF sputtering deposition process of hydrogen-doped indium oxide using a gas mixture of Ar/H_2 and pulsed oxygen, and investigated its effect on the opto-electronic properties, namely the Rsh and AVT, of as-deposited and annealed IOH films.

The oxygen partial pressure influences the optical and electrical properties. Despite influencing the detailed spectral shape of the transmittance, there is no significant impact on the AVT. The sheet resistance shows a non-linear dependence on $p(O_2)$, with the lowest Rsh achieved at $p(O_2)$ at 3.2×10^{-2} Pa. The use of Ar/H_2 gas mixture is a suitable H-doping alternative, with an optimum $p(Ar/H_2)$ of 13×10^{-2} Pa, leading to a Rsh after annealing of 19

Ohm/sq. Another key parameter is the thickness and consequentially, the process duration, since thicker films lead to lower sheet resistance. Overall, the films' AVT presented no significant changes, remaining between 87 – 89 % regardless of the deposition conditions.

To obtain a film with the desired requirements, it is necessary to find a balance between oxygen, Ar/H_2 and thickness. Further investigation of the IOH film's structural, electrical, and optical properties is required, as is it's use as a transparent back contact in semi-transparent CIGS solar cells.

Acknowledgments

This work was supported by the project "Semi-Transparent Solar cells for building integrated photovoltaics (STAR-SOL)", funded by FCT – Fundação para a Ciência e a Tecnologia (FCT-FNR/0001/2018). Marina Alves thanks the Fundação para a Ciência e a Tecnologia (FCT), Portugal for the PhD Grant (2020.06063.BD).

References

[1] J. Sun, J.J. Jasieniak, Semi-transparent solar cells, J. Phys. D. Appl. Phys. 50 (2017) 093001. https://doi.org/10.1088/1361-6463/aa53d7.

[2] M.A. Green, E.D. Dunlop, J. Hohl-Ebinger, M. Yoshita, N. Kopidakis, A.W.Y. Ho-Baillie, Solar cell efficiency tables (Version 55), Prog. Photovoltaics Res. Appl. 28 (2020) 3–15. https://doi.org/10.1002/pip.3228.

[3] J. Ramanujam, U.P. Singh, Copper indium gallium selenide based solar cells - A review, Energy Environ. Sci. 10 (2017) 1306–1319. https://doi.org/10.1039/c7ee00826k.

[4] T.D. Lee, A.U. Ebong, A review of thin film solar cell technologies and challenges, Renew. Sustain. Energy Rev. 70 (2017) 1286–1297. https://doi.org/10.1016/j.rser.2016.12.028.

[5] M. Saifullah, S. Ahn, J. Gwak, S. Ahn, K. Kim, J. Cho, J.H. Park, Y.J. Eo, A. Cho, J.-S. Yoo, J.H. Yun, Development of semitransparent CIGS thin-film solar cells modified with a sulfurized-AgGa layer for building applications, J. Mater. Chem. A. 4 (2016) 10542–10551. https://doi.org/10.1039/C6TA01909A.

[6] J. Keller, N. Shariati Nilsson, A. Aijaz, L. Riekehr, T. Kubart, M. Edoff, T. Törndahl, Using hydrogen-doped In2O3 films as a transparent back contact in (Ag,Cu)(In,Ga)Se2 solar cells, Prog. Photovoltaics Res. Appl. 26 (2018) 159–170. https://doi.org/10.1002/pip.2977.

[7] J. Keller, W.-C. Chen, L. Riekehr, T. Kubart, T. Törndahl, M. Edoff, Bifacial Cu(In,Ga)Se2 solar cells using hydrogen-doped In2O3 films as a transparent back contact, Prog. Photovoltaics Res. Appl. 26 (2018) 846–858.

https://doi.org/10.1002/pip.3025.

[8] T. Koida, H. Fujiwara, M. Kondo, Hydrogen-doped In2O3 as High-mobility Transparent Conductive Oxide, Jpn. J. Appl. Phys. 46 (2007) L685–L687. https://doi.org/10.1143/JJAP.46.L685.

[9] T. Koida, H. Shibata, M. Kondo, K. Tsutsumi, A. Sakaguchi, M. Suzuki, H. Fujiwara, Correlation between oxygen stoichiometry, structure, and opto-electrical properties in amorphous In 2 O 3 :H films, J. Appl. Phys. 111 (2012) 063721. https://doi.org/10.1063/1.3696978.

[10] T. Jäger, Y.E. Romanyuk, S. Nishiwaki, B. Bissig, F. Pianezzi, P. Fuchs, C. Gretener, M. Döbeli, A.N. Tiwari, Hydrogenated indium oxide window layers for high-efficiency Cu(In,Ga)Se2 solar cells, J. Appl. Phys. 117 (2015) 205301. https://doi.org/10.1063/1.4921445.

[11] S. Mandal, A. Pandey, V.K. Komarala, Investigation of optoelectrical properties of indium oxide thin films with hydrogen and oxygen gas concentration variation during sputtering, Mater. Sci. Semicond. Process. 123 (2021) 105576. https://doi.org/10.1016/j.mssp.2020.105576.

[12] T. Koida, M. Kondo, K. Tsutsumi, A. Sakaguchi, M. Suzuki, H. Fujiwara, Hydrogen-doped In2O3 transparent conducting oxide films prepared by solid-phase crystallization method, J. Appl. Phys. 107 (2010) 033514. https://doi.org/10.1063/1.3284960.

[13] T. Koida, H. Fujiwara, M. Kondo, Reduction of Optical Loss in Hydrogenated Amorphous Silicon/Crystalline Silicon Heterojunction Solar Cells by High-Mobility Hydrogen-Doped In2O3 Transparent Conductive Oxide, Appl. Phys. Express. 1 (2008) 041501. https://doi.org/10.1143/APEX.1.041501.

[14] T. Koida, H. Fujiwara, M. Kondo, High-mobility hydrogen-doped In2O3 transparent conductive oxide for a-Si:H/c-Si heterojunction solar cells, Sol. Energy Mater. Sol. Cells. 93 (2009) 851–854. https://doi.org/10.1016/j.solmat.2008.09.047.

[15] L. Barraud, Z.C. Holman, N. Badel, P. Reiss, A. Descoeudres, C. Battaglia, S. De Wolf, C. Ballif, Hydrogen-doped indium oxide/indium tin oxide bilayers for high-efficiency silicon heterojunction solar cells, Sol. Energy Mater. Sol. Cells. 115 (2013) 151–156. https://doi.org/10.1016/j.solmat.2013.03.024.

[16] S. Li, Z. Shi, Z. Tang, X. Li, Study on the hydrogen doped indium oxide for silicon heterojunction solar cell application, J. Alloys Compd. 705 (2017) 198–204. https://doi.org/10.1016/j.jallcom.2017.02.133.

[17] J. Keller, A. Aijaz, F. Gustavsson, T. Kubart, L. Stolt, M. Edoff, T. Törndahl, Direct comparison of atomic layer deposition and sputtering of In2O3:H used as transparent conductive oxide layer in CuIn1−xGaxSe2 thin film solar cells, Sol. Energy Mater. Sol. Cells. 157 (2016) 757–764. https://doi.org/10.1016/j.solmat.2016.07.012.

[18] M. Boccard, N. Rodkey, Z.C. Holman, High-mobility Hydrogenated Indium Oxide without Introducing Water During Sputtering, Energy Procedia. 92 (2016) 297–303. https://doi.org/10.1016/j.egypro.2016.07.083.

List of Figures

Credit author statement

Marina Alves: Conceptualization, Methodology, Formal analysis, Investigation, Writing – original draft, Writing – review and editing;
Daniel Brito: Methodology, Formal analysis, Writing – review and editing
Joaquim Carneiro: Methodology, Writing – review and editing
Vasco Teixeira: Methodology, Writing – review and editing
Sascha Sadewasser: Conceptualization, Methodology, Investigation, Writing – review and editing, Project Administration, Funding acquisition.

Declaration of interests

☒The authors declare that they have no known competing financial interests or personal relationships that could have appeared to influence the work reported in this paper.

☐The authors declare the following financial interests/personal relationships which may be considered as potential competing interests: